

inwards by angular momentum exchange with a protoplanetary disk (which initially extends inward nearly to the star). This migration could transfer material from the inner part of the disk to the outer part. The mass enhancement of the outer disk should be related to the angular momentum lost from the planet. Our observations are consistent with a circumstellar disk ten times more massive than our own, consistent with transfer of angular momentum from a migrating planet to the outer disk. Furthermore, the disk of material around 55 Cnc shows an extent consistent with what is expected for our own Kuiper Belt, and a spectral similarity to that expected for our Kuiper Belt. Unlike our Kuiper Belt, a disk around another star can be studied globally to determine its mass, composition and radial structure. Further study of this and other circumstellar disks will allow the characterization of global properties and will in turn lead to an increased understanding of our own Kuiper Belt. □

Received 3 April; accepted 9 July 1998.

- Butler, R. P., Marcy, G. W., Williams, E., Hauser, H. & Shirts, P. Three new '51 Pegasi-type' planets. *Astrophys. J.* **474**, L115–L118 (1997).
- Dominik, C., Laureijs, R. J., Jourdan de Muizon, M. & Habing, H. J. A Vega-like disk associated with the planetary system of ρ^1 Cnc. *Astron. Astrophys.* **329**, L53–L56 (1998).
- Weissman, P. The Kuiper belt. *Annu. Rev. Astron. Astrophys.* **33**, 327–358 (1995).
- The Hipparcos and Tycho Catalogues* (European Space Agency, Noordwijk, The Netherlands, 1997).
- Smith, B. A. & Terrile, R. J. A circumstellar disk around β Pictoris. *Science* **226**, 1421–1424 (1984).
- Brown, R. H., Cruikshank, D. P., Pendleton, Y. & Veeder, G. J. Surface composition of Kuiper belt object 1993SC. *Science* **276**, 937–939 (1997).
- Mannings, V., Koerner, D. W. & Sargent, A. I. A rotating disk of gas and dust around a young counterpart to β Pictoris. *Nature* **388**, 555–557 (1997).
- Duncan, M. J. & Levison, H. F. A disk of scattered icy objects and the origin of Jupiter-family comets. *Science* **276**, 1670–1672 (1997).
- Owen, T. C. *et al.* Surfaces and the atmospheric composition of Pluto. *Science* **261**, 745–748 (1993).
- Lewis, J. S. *Physics and Chemistry of the Solar System* (Academic, San Diego, 1995).
- Luu, J. X. & Jewitt, D. C. Reflection spectrum of the Kuiper belt object 1993 SC. *Astron. J.* **111**, 499–503 (1996).
- Jewitt, D. C., Luu, J. X. & Chen, J. The Mauna Kea–Cerro Tololo (MKCT) Kuiper belt and centaur survey. *Astron. J.* **112**, 1225–1238 (1996).
- Farinella, P. & Davis, D. R. Short-period comets: primordial bodies or collisional fragments? *Science* **273**, 938–941 (1996).
- Dohnanyi, J. S. Collisional model of asteroids and their debris. *J. Geophys. Res.* **74**, 2531–2554 (1969).
- Lin, D. N. C., Bodenheimer, P. & Richardson, D. C. Orbital migration of the planetary companion of 51 Pegasi to its present location. *Nature* **380**, 606–607 (1996).
- Trilling, D. E. *et al.* Orbital evolution and migration of giant planets: modeling extrasolar planets. *Astrophys. J.* **500**, 428–439 (1998).
- Murray, N., Hansen, B., Holman, M. & Tremaine, S. Migrating planets. *Science* **279**, 69–72 (1998).
- Duncan, M. J., Levison, H. F. & Budd, S. M. The dynamical structure of the Kuiper belt. *Astron. J.* **110**, 3073–3081 (1995).
- Malhotra, R. The origin of Pluto's peculiar orbit. *Nature* **365**, 819–821 (1993).

Acknowledgements. We thank Doug Toomey for instrumental assistance, and Andy Rivkin for many useful discussions. D.E.T. and R.H.B. were visiting astronomers at the Infrared Telescope Facility which is operated by the University of Hawaii under contract to the National Aeronautics and Space Administration. This work is supported in part by an NSF Graduate Research Fellowship and by various NASA research grants.

Correspondence should be addressed to D.E.T. (e-mail: trilling@lpl.arizona.edu).

Induced magnetic fields as evidence for subsurface oceans in Europa and Callisto

K. K. Khurana*, M. G. Kivelson*†, D. J. Stevenson‡, G. Schubert*†, C. T. Russell*†, R. J. Walker* & C. Polansky‡

* Institute of Geophysics and Planetary Physics, † Department of Earth and Space Sciences, University of California, Los Angeles, California 90095, USA

‡ Division of Geological and Planetary Sciences, California Institute of Technology, Pasadena, California 91125, USA

§ The Jet Propulsion Laboratory, 4800 Oak Grove Road, Pasadena, California 91109, USA

The Galileo spacecraft has been orbiting Jupiter since 7 December 1995, and encounters one of the four galilean satellites—Io, Europa, Ganymede and Callisto—on each orbit. Initial results from the spacecraft's magnetometer^{1,2} have indicated that neither Europa nor Callisto have an appreciable internal magnetic field, in

contrast to Ganymede³ and possibly Io⁴. Here we report perturbations of the external magnetic fields (associated with Jupiter's inner magnetosphere) in the vicinity of both Europa and Callisto. We interpret these perturbations as arising from induced magnetic fields, generated by the moons in response to the periodically varying plasma environment. Electromagnetic induction requires eddy currents to flow within the moons, and our calculations show that the most probable explanation is that there are layers of significant electrical conductivity just beneath the surfaces of both moons. We argue that these conducting layers may best be explained by the presence of salty liquid-water oceans, for which there is already indirect geological evidence^{5,6} in the case of Europa.

Our insight into the source of the magnetic perturbations

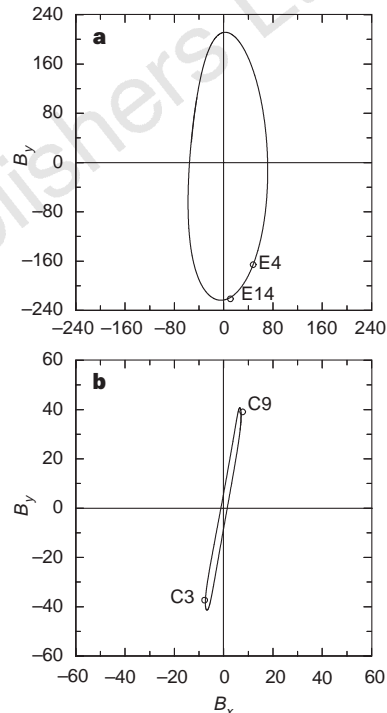


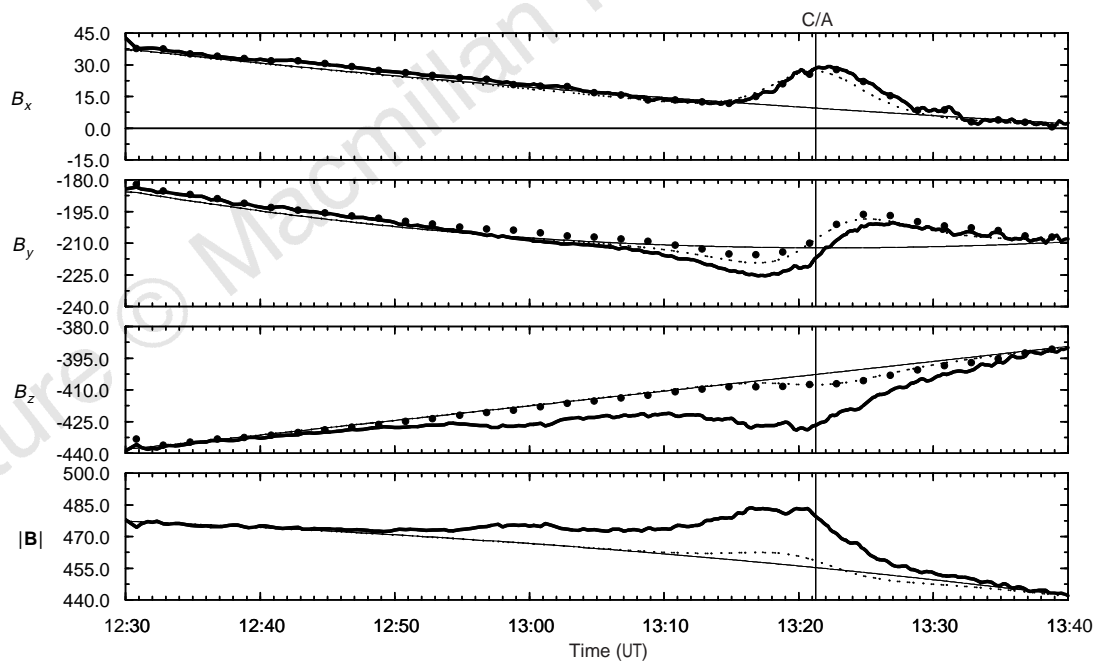
Figure 1 The varying magnetic fields experienced by Europa and Callisto. Near the orbits of the satellites (the orbits of Europa and Callisto lie nearly in Jupiter's spin equator at $9.4R_J$ and $26.3R_J$, respectively) but remote from the actual satellite locations, the sources of magnetic field are the internal tilted dipole of Jupiter and the currents flowing in the magnetospheric plasma sheet. The 9.6° tilt between Jupiter's spin and dipole axes implies that the magnetic equatorial plane and the orbital planes of the moons are inclined relative to each other. In a coordinate system with the x axis along the direction of plasma co-rotation, the y axis orientated towards Jupiter, and the z axis along the spin axis of the moon, the z component remains essentially constant. However, the x and y components of the magnetospheric field vary at the synodic period of Jupiter's rotation (11.1 h for Europa and 10.1 h for Callisto) as illustrated in the plots. **a**, The elliptically polarized variation of the magnetic field (in nT) at Europa. Open circles mark the field values corresponding to the E4 and E14 fly-bys. **b**, The almost linearly polarized variation of the magnetic field (in nT) at Callisto. Open circles mark the field values corresponding to the C3 and C9 fly-bys. The time, altitude and latitude relative to the moon's equator for the four passes were: E4, 1996 December 19 06:52:58 UT, 688.1 km, -1.6° ; E14, 1998 March 29 13:21:16 UT, 1,641.3 km, 12.0° ; C3, 1996 November 04 13:24:28 UT, 1,138.9 km, 13.2° ; C9, 1997 June 25 13:47:50 UT, 421.0 km, 2.0° . At the times of these encounters, the SIII west longitude and position relative to the jovian plasma sheet were: E4, 156.8° , $\sim 1R_J$ above; E14, 184.4° , $\sim 1R_J$ above; C3, 242.9° , $\sim 1R_J$ above; C9, 59.9° , $\sim 1R_J$ below ($R_J \equiv$ radius of Jupiter = 71,492 km). The expected background field was calculated from an empirical model of Jupiter's magnetospheric field that uses spherical harmonics of order 3 to describe the internal field³² and an Euler potential formulation³³ to describe the external field from the current sheet.

recorded near the moons is based on data from four passes for which the signal (induction signature) to noise (perturbations generated within the ambient magnetospheric plasma) ratio is large. Further details of the results from these and other Europa and Callisto fly-bys will appear elsewhere³⁴. Europa and Callisto are located in the inner magnetosphere of Jupiter, where the plasma is confined to a thin sheet (half thickness $\sim 2 R_J$, where R_J is the radius of Jupiter) near the dipole equator. Jupiter's strong magnetic field keeps the ambient plasma close to rigid co-rotation with Jupiter, implying that it overtakes the orbiting moons from behind. In the rest frame of the moons, the magnetospheric field wobbles as shown in Fig. 1. A varying magnetic field with a peak amplitude of ~ 220 nT (~ 40 nT) is imposed on Europa (Callisto) at the synodic period (the period observed in the moon's rest frame) of Jupiter's rotation. Conductors within or surrounding the moons respond to such varying fields by generating eddy currents on their surfaces. In a uniform oscillating field, eddy currents on the surface of a highly conducting sphere or a spherical shell generate the field of an oscillating magnetic dipole external to the conductor and cancel the oscillating field inside the conductor⁷. Continuity of the normal component of the magnetic field requires that at the pole of the induced dipole, the induced field cancel the background field.

The interactions of the moons with the magnetospheric plasma perturb the background field thereby complicating the interpretation of the induction signature. At Europa, the principal plasma

effect comes from the mass loading of the plasma from newly picked-up water group ions. Such an interaction enhances the field strength upstream of the moon and decreases it downstream of the moon. Other plasma-related effects that obscure the induction signature include the standing Alfvén wave current system that flows through an external conducting layer⁸ surrounding the moon (an ionosphere, for example), diamagnetism from newly picked-up plasma, an expansion fan introduced in the wake of a non-conducting moon by the absorption of plasma by the moon⁹, and the ambient ultra-low frequency (ULF) waves present in the plasma sheet of Jupiter¹⁰. To minimize the complications arising from the plasma effects, we have concentrated on two of the Europa fly-bys (orbits E4 and E14) and two of the Callisto fly-bys (orbits C3 and C9) for which the moons were located outside the central dense part of Jupiter's plasma sheet. For these passes, the moon-plasma interaction was weak and the background fluctuations from ULF waves were small.

Figure 2 shows data from encounter E14. (See Fig. 1 and Fig. 1 legend for parameters of this and other encounters.) Also plotted are the predictions from the induction model (with no adjustable parameters). Near the equatorial plane of Europa, where these observations were made, induction is not expected to modify greatly the component of the magnetic field in the z -direction, B_z . We believe that the field magnitude and B_z are enhanced during this and other Europa encounters principally by mass loading¹¹, diversion



x	-9.84	-8.17	-6.56	-4.95	-3.31	-1.65	0.04	1.75
y	8.06	6.16	4.34	2.51	0.67	-1.16	-2.96	-4.72
z	0.28	0.31	0.34	0.37	0.39	0.41	0.42	0.43
R	12.72	10.24	7.87	5.56	3.40	2.06	2.99	5.05

Figure 2 Magnetic field observations for the E14 pass. The plot covers a time interval of 70 min during which the spacecraft moved inward from an initial range of $13 R_E$ to $\sim 2 R_E$ at closest approach (C/A), and travelled back out to a distance of $5 R_E$ from Europa (here R_E is the radius of Europa). The observed magnetic field components and magnitude (in nT) are plotted as thick solid lines. The thin solid lines represent the estimated background field of Jupiter's magnetosphere along Galileo's trajectory, estimated from the interpolation of magnetic data obtained along the trajectory when the spacecraft was sufficiently far from Europa ($>12 R_E$) that the induction and plasma interaction effects were negligible. The modelled field (induction + background) is shown by dotted lines, and provides a satisfactory fit to the large-scale field variations. Filled circles

show the observations corrected for the plasma pick-up effect described in the text, and this correction is seen to improve the agreement. The variables x , y and z shown under the figure describe the trajectory of the spacecraft in the coordinate system described in Fig. 1 legend. R is the range of the spacecraft. All distances are in units of R_E ($1 R_E =$ radius of Europa = 1,560 km). The data sampling rate changes from 25 s to 1 s at 13:05:40 UT. The induced model field used here and in Fig. 3 was calculated using the equations $B_r = B_0(t)(1 - (a/r)^3)\cos\theta$, $B_\theta = B_0(t)(1 + 0.5(a/r)^3)\sin\theta$, $B_\phi = 0$, where B_r , B_θ and B_ϕ are the components of magnetic field in a spherical coordinate system which has a pole direction antiparallel to the background field, B_0 .

of flow by the conducting obstacle and associated plasma effects. As the component of the magnetic field (B_x) along the flow direction is small ($B_x/|\mathbf{B}| \ll 1$) for all the encounters, plasma effects will be symmetric about a plane through the centre of the moon perpendicular to the background magnetic field. Above and below this plane, plasma currents drape the field around the moon, causing bending. In the symmetry plane, near which these observations were made, plasma effects change the field strength without changing its orientation. If the orientation of the field is not to change, each component must change by the same fractional amount: $\delta B_x/B_x \approx \delta B_y/B_y \approx \delta B_z/B_z \approx \delta|\mathbf{B}|/|\mathbf{B}|$. Here $\delta|\mathbf{B}|$ is the change in the field strength. Thus, by reducing each component by a factor $(1 - \delta|\mathbf{B}|/|\mathbf{B}|)$, we can approximately remove the plasma contributions. The correction improves the agreement between the observations and the model for both the E14 and E4 (not shown here) fly-bys.

At Callisto, corrections for plasma effects are not needed. Figure 3 shows the observed perturbations and the induced dipole model for the C3 and C9 passes: agreement is good. As these Callisto encounters occurred at opposite phases of the variation of the background field (away from Jupiter for the C3 fly-by and towards Jupiter for C9), the induced dipole moments were roughly antiparallel (see Fig. 3a and b). This convincingly demonstrates that the Callisto observations cannot be explained by a fixed internal dipole. For the multiple Europa observations, the orientation of the time-varying component of Jupiter's field changed only slightly among the relevant passes, so the induced dipole moments differed only slightly. A fixed internal dipole cannot be excluded, although its orientation at a large angle to the spin axis seems improbable.

The induced-field model for Europa and Callisto constrains their interior structures by requiring conducting paths at or near the surfaces. It is known that a periodically varying magnetic field (angular frequency ω) acting on an electrically conducting object of conductivity σ decays in an e-folding length of $S = (\omega\mu\sigma/2)^{-1/2}$; here S is the skin depth and μ is the permeability. If the period of the

wave is 11 h and the conductivity is 1 S m^{-1} , $S \approx 95 \text{ km}$. The solution for a spherical shell can be expressed in terms of Bessel functions, but when the thickness of the conducting layer is $\geq 0.1 S$ and $S \ll a$ with a the radius of the conductor, the solution outside the conductor is the sum of an induced dipole field (whose surface field at the pole is equal and opposite to the background field) and the uniform background field⁷ (see Fig. 2 legend).

The observed amplitudes of the induced signatures of Europa and Callisto require conducting layers of depth $>0.1 S$ near the surfaces. For Europa, an obvious candidate for conducting paths is its ionosphere¹² or a cloud of pickup ions¹³. However, estimates of the conductivity above the surface give skin depths for a ten-hour wave much larger than the moon itself. Thus the wave easily penetrates the ionosphere without causing significant induction. Skin depths (for an approximately ten-hour wave) of various materials likely to be found in the icy outer layers of Europa or Callisto can be determined. A rocky mantle composed of (pure) ice and rocks would have a skin depth greater than 10^6 km . Metals such as iron are not expected to be abundant in the outer layers of a differentiated body. Induction from inner metallic cores can also be ruled out. A metallic core whose radius is half the moon's radius would produce a signature that is only one-eighth as large as observed because the induced dipole field magnitude falls as inverse distance cubed. An ocean whose salinity is comparable with Earth's ocean could produce the signature. The conductivity of Earth's ocean water¹⁴ (salinity 3.75%) is $\sim 2.75 \text{ S m}^{-1}$ at 0°C . Thus Earth-like oceans with thicknesses $>10 \text{ km}$ could generate the observed signatures in Europa and Callisto. The conductivity of ocean water is electrolytic and requires only small amounts (a few per cent) of dissolved salts (like NaCl) or acids (like H_2SO_4) that hydrolyse readily.

Induced fields at Europa have been considered since 1985¹⁵, followed by more recent speculations¹⁶. Neubauer¹³ noted that the published^{1,2} dipole moments of the magnetic field perturbations near Europa and Callisto could be fully or partially explained by induction from subsurface oceans or dirty ice layers near the melting point.

The possibility of a liquid-water ocean beneath the icy surface of Europa has been debated for more than two decades. Accretional and radiogenic heat sources are large enough to dehydrate the interior of Europa early in its evolution, leaving the moon covered with a layer of liquid water $\geq 100 \text{ km}$ thick¹⁷. Measurements by the spacecraft Galileo of Europa's gravitational field show that Europa is strongly differentiated (with a metallic core), and that it indeed has a water ice-liquid outer layer $\sim 100 \text{ km}$ thick¹⁸.

Early thermal models considered only the conductive cooling and freezing with time of the outer layer of water, and predicted that at present liquid water existed beneath an ice shell. It was later shown¹⁹ that with thickening, the outer layer of ice would become unstable to thermal convection, promoting heat transfer through the ice and solidification of the underlying water. Complete freezing of the outer layer of water in a small fraction of geological time is possible but not certain²⁰, even for pure water. Additionally, tidal dissipation in Europa's ice shell provides a heat source that could offset the convective cooling of the ice and prevent complete solidification of the water ocean²¹.

The competition between the tendency of tidal heating to maintain a liquid water ocean and that of ice convection to freeze the ocean has been analysed, but a definitive conclusion was not reached²²⁻²⁴. Significant uncertainties include the unknown rheology of ice²⁵ and the dependence of the thermal conductivity of ice on its temperature and physical state. A thermally insulating surface layer would promote stabilization of a liquid-water ocean²³. The occurrence of minor constituents in the ice and ocean, such as salts²⁶ and ammonia, would affect the rheology of the ice and the freezing temperature of the ocean. Tidal heating of the main faults in the ice²⁷ and frictional dissipation due to forced circulation in a thin liquid-water ocean may be important.

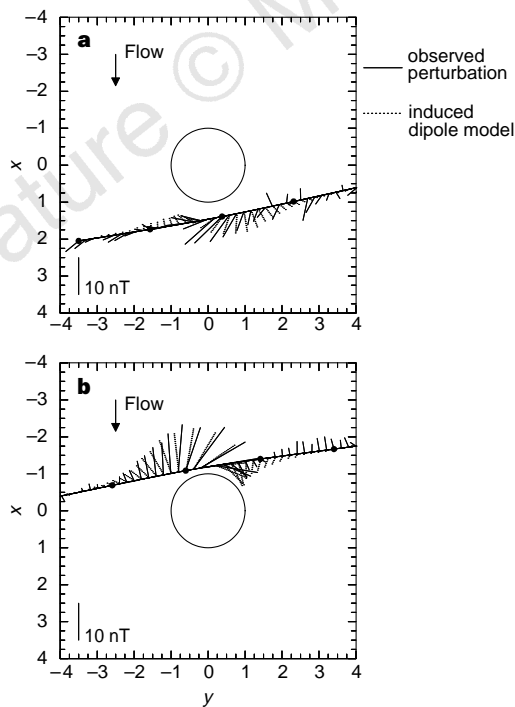


Figure 3 Magnetic field observations from the C3 and C9 passes. **a**, The magnetic field perturbations (vectors drawn with solid lines) and the modelled induction field (vectors shown dotted) along the trajectory of the C3 encounter in the x - y plane. **b**, The magnetic field perturbations and the modelled induction field for the C9 encounter. The distance scale is in units of R_C ($1R_C =$ radius of Callisto = 2,409 km).

Whereas the possible existence of a liquid-water ocean on Europa is plausible, the opposite is true for Callisto. Callisto consists of roughly equal amounts of rock and ice. It is not tidally heated, there is no geological evidence for significant endogenic modification of its surface, and gravity measurements by the Galileo spacecraft show only partial separation of the ice and rock in its interior²⁸. These observations are consistent with little modification of Callisto since its accretion. We note that thermal models of Callisto give no hint of a subsurface liquid-water ocean¹⁷. Accretional and radiogenic heating are marginally able to separate the ice and rock inside Callisto, but the present gravitational evidence shows that unlike Ganymede²⁹ separation has been incomplete: Callisto has not been heated enough to have melted all its ice.

Is it possible for some of the ice in the outer part of Callisto to have melted, and could a near-surface liquid-water layer be prevented from freezing? Because accretional heating is largest when a planet is near maximum size, we consider that it is possible for the ice to have melted in the outer layers of Callisto. More problematic is keeping such a layer from freezing; tidal heating is necessary for the maintenance of a liquid ocean on Europa, and there is no tidal heating on Callisto. The presence of 'antifreeze' (salts or ammonia) would help. The layer needs to have substantial thickness, and for this reason an ocean separating two solid convecting regions is most plausible. The possibility of a liquid-water ocean in Callisto is startling, but we have no other explanation for the near-surface highly electrically conducting layer required by the observed induction signal. Of the two icy galilean satellites, it would be more plausible for Ganymede to have a subsurface liquid-water ocean. Ganymede is completely differentiated; extensive endogenic modification of its surface and the existence of an intrinsic magnetic field³ imply a dynamic interior in the past, and possibly also in the present³⁰. Perhaps Ganymede also has an internal liquid-water ocean if Callisto has one, but Ganymede's intrinsic magnetic field obscures any induction signal.

One possible source of heat not yet considered is ohmic heating by the eddy currents in the moons. The dissipated power can be estimated from the expression³¹ $\text{power/area} = \omega B^2/4\mu_0$, which is the ohmic loss from a propagating electromagnetic wave in a conducting waveguide (here μ_0 is the permeability of vacuum). Multiplication by the surface area of the moon and substitution of varying field amplitudes of 220 nT (Europa) and 40 nT (Callisto) gives 5×10^6 (S/100 km) W for Europa and 4×10^5 (S/100 km) W for Callisto; nominal values for S are of the order of 100 km. More rigorous estimates would not change the conclusion that the heat input from this source is negligible.

We conclude from an analysis of the magnetic field observations that it is very likely that both Europa and Callisto possess internal salty liquid-water oceans. In the case of Europa, this conclusion is supported by indirect geological evidence^{5,6}. □

Received 24 June; accepted 14 August 1998.

- Kivelson, M. G. *et al.* Europa's magnetic signature: report from Galileo's first pass on December 19, 1996. *Science* **276**, 1239–1241 (1997).
- Khurana, K. K., Kivelson, M. G., Russell, C. T., Walker, R. J. & Southwood, D. J. Absence of an internal magnetic field at Callisto. *Nature* **387**, 262–264 (1997).
- Kivelson, M. G. Discovery of Ganymede's magnetic field by the Galileo spacecraft. *Nature* **384**, 537–541 (1996).
- Kivelson, M. G. *et al.* A magnetic signature at Io: initial report from the Galileo magnetometer. *Science* **273**, 337–340 (1996).
- Carr, M. H. *et al.* Evidence for a subsurface ocean on Europa. *Nature* **391**, 363–365 (1998).
- Pappalardo, R. T. *et al.* Geological evidence for solid-state convection in Europa's ice shell. *Nature* **391**, 365–368 (1998).
- Parkinson, W. D. *Introduction to Geomagnetism* 308–340 (Scottish Academic, Edinburgh, 1993).
- Neubauer, F. M. Nonlinear standing Alfvén wave current system at Io: Theory. *J. Geophys. Res.* **85**, 1171–1178 (1980).
- Owen, C. J. *et al.* The lunar wake at 6.8 R_J : WIND magnetic field observations. *Geophys. Res. Lett.* **23**, 1263–1266 (1996).
- Khurana, K. K. & Kivelson, M. G. Ultra low frequency MHD waves in Jupiter's middle magnetosphere. *J. Geophys. Res.* **94**, 5241–5254 (1989).
- Ip, W.-H. Europa's oxygen exosphere and its magnetospheric interaction. *Icarus* **120**, 317–325 (1996).
- Kliore, A. J., Hinson, D. P., Flasar, F. M., Nagy, A. F. & Cravens, T. E. The ionosphere of Europa from Galileo radio occultations. *Science* **277**, 355–358 (1997).
- Neubauer, F. M. The subalfvénic interaction of the Galilean satellites with the Jovian magnetosphere. *J. Geophys. Res. (Planets)* **103**, 19843–19866 (1998).

- Montgomery, R. B. in *American Institute of Physics Handbook* 125–127 (McGraw Hill, New York, 1963).
- Colburn, D. S. & Reynolds, R. T. Electrolytic currents in Europa. *Icarus* **63**, 39–44 (1985).
- Kargel, J. S. & Consolmagno, G. J. Magnetic fields and the detectability of brine oceans in Jupiter's icy satellites. *Lunar Planet. Sci. Conf. XXVII*, 643–644 (1996).
- Schubert, G., Spohn, T. & Reynolds, R. in *Satellites* (eds Burns, J. A. & Matthews, M. S.) 224–292 (Univ. Arizona Press, Tucson, 1986).
- Anderson, J. D. Europa's differentiated internal structure: inferences from four Galileo encounters. *Science* (in the press).
- Reynolds, R. T. & Cassen, P. On the internal structure of the major satellites of the outer planets. *Geophys. Res. Lett.* **6**, 121–124 (1979).
- Kirk, R. L. & Stevenson, D. J. Thermal evolution of a differentiated Ganymede and implications for surface features. *Icarus* **69**, 91–135 (1987).
- Cassen, P. M., Reynolds, R. T. & Peale, S. J. Is there liquid water on Europa? *Geophys. Res. Lett.* **6**, 731–734 (1979).
- Squyres, S. W., Reynolds, R. T., Cassen, P. M. & Peale, S. J. Liquid water and active resurfacing on Europa. *Nature* **301**, 225–226 (1983).
- Ross, M. N. & Schubert, G. Tidal heating in an internal ocean model of Europa. *Nature* **325**, 133–134 (1987).
- Ojakangas, G. W. & Stevenson, D. J. Thermal state of an ice shell on Europa. *Icarus* **81**, 220–241 (1989).
- Durham, W. B., Kirby, S. H. & Stern, L. A. Creep of water ices at planetary conditions: a compilation. *J. Geophys. Res.* **102**, 16293–16302 (1997).
- McCord, T. B. *et al.* Salts on Europa's surface detected by Galileo's Near Infrared Mapping Spectrometer. *Science* **280**, 1242–1245 (1998).
- Stevenson, D. J. in *Proc. Europa Conf.* 69–70 (San Juan Capistrano Research Inst., San Juan Capistrano, CA, 1996).
- Anderson, J. D. *et al.* Distribution of rock, metals, and ices in Callisto. *Science* **280**, 1573–1576 (1998).
- Anderson, J. D., Lau, E. L., Sjogren, W. L., Schubert, G. & Moore, W. B. Gravitational constraints on the internal structure of Ganymede. *Nature* **384**, 541–543 (1996).
- Schubert, G., Zhang, K., Kivelson, M. G. & Anderson, J. D. The magnetic field and internal structure of Ganymede. *Nature* **384**, 544–545 (1996).
- Jackson, J. D. *Classical Electrodynamics* 2nd edn 338 (Wiley, New York, 1975).
- Connerney, J. E. P. Magnetic fields of the outer planets. *J. Geophys. Res.* **98**, 18659–18679 (1993).
- Khurana, K. K. Euler potential models of Jupiter's magnetospheric field. *J. Geophys. Res.* **102**, 11295–11306 (1997).
- M. G. Kivelson *et al.* Europa and Callisto; induced or intrinsic fields in a periodically varying plasma environment. *J. Geophys. Res.* (submitted).

Acknowledgements. We thank D. Bindschadler of the Jet Propulsion Laboratory for support in all phases of data collection and J. Mafi for data processing and preparation of data plots. This work was partially supported by the Jet Propulsion Laboratory.

Correspondence and requests for materials should be addressed to K.K.K. (e-mail: kkhurana@igpp.ucla.edu).

Quantized conductance through individual rows of suspended gold atoms

Hideaki Ohnishi*, Yukihito Kondo* & Kunio Takayanagi†

* Takayanagi Particle Surface Project, ERATO, Japan Science and Technology Corporation, 3-1-2 Musashino, Akishima, Tokyo 196, Japan

† Department of Material Science and Engineering, Tokyo Institute of Technology, 4259 Nagatsuta, Midori-ku, Yokohama, Kanagawa 226, Japan

As the scale of microelectronic engineering continues to shrink, interest has focused on the nature of electron transport through essentially one-dimensional nanometre-scale channels such as quantum wires¹ and carbon nanotubes^{2,3}. Quantum point contacts (QPCs) are structures (generally metallic) in which a 'neck' of atoms just a few atomic diameters wide (that is, comparable to the conduction electrons' Fermi wavelength) bridges two electrical contacts. They can be prepared by contacting a metal surface with a scanning tunnelling microscope (STM)^{4–7} and by other methods^{8–12}, and typically display a conductance quantized in steps of $2e^2/h$ ($\sim 13 \text{ k}\Omega^{-1}$)^{13,14}, where e is the electron charge and h is Planck's constant. Here we report conductance measurements on metal QPCs prepared with an STM that we can simultaneously image using an ultrahigh-vacuum electron microscope, which allows direct observation of the relation between electron transport and structure. We observe strands of gold atoms that are about one nanometre long and one single chain of gold atoms suspended between the electrodes. We can thus verify that the conductance of a single strand of atoms is $2e^2/h$ and that the conductance of a double strand is twice as large, showing that